

ON THE MAIN PROPERTIES OF THE PRIMAL–MIXED FINITE ELEMENT FORMULATION

M. Berkoviæ, D. Mijuca

Faculty of Mathematics, University of Belgrade, Studentski trg 16, P.O. Box 550, 11000 Belgrade, Yugoslavia
e-mail: dmijuca@matf.bg.ac.yu

Abstract. *In the present paper the main properties of the coordinate independent finite element primal–mixed formulation based on the stationary Reissner's principle, having both the displacement and stress boundary conditions exactly satisfied and solvable by direct Gaussian elimination procedure, are presented. From the presented numerical results it can be concluded that the proposed procedure is easy for implementation, stable even in the presence of singularities and more efficient, in the sense of the execution time needed for the prescribed accuracy, than classical displacement finite element method.*

1. INTRODUCTION

Mixed finite element methods, in the mechanics of solids, are based on formulations having also stresses and/or strains as fundamental variables, at variance with the classical (primal) finite element method where fundamental unknowns are only displacements. There are opinions [1] that mixed methods have some serious drawbacks. For instance, a fact that discrete mixed system involves more degrees of freedom than a primal one, and hence the unacceptable execution time for the *same mesh*, is considered as one of main disadvantages of mixed methods. In this paper we show that the present mixed model is faster than classical finite element analysis for the *same accuracy*. Further, the classical approach, based on an extremum principle of the minimum of the potential energy, has a positive definite system matrix. On the contrary, as a saddle point problem, mixed approach leads to an indefinite system of algebraic equations, thus narrowing the number of solution techniques that can be applied directly. However, a usual sparse Gaussian elimination solver can be, and has been, successfully used for the solution of the resulting systems of equations of the proposed procedure. Finally, at variance with some other closely related procedures it has been shown by numerical examples that the present approach can be rendered stable in the presence of singularities.

The most frequent motivation for the use of mixed methods is their robustness in the presence of certain limiting and extreme situations [1], as the problem of incompressibility or locking are. The main goal of the present paper is however to reconsider the use of mixed formulation as a tool for wider application, i.e. to study the stability accuracy and efficiency of a procedure using examples otherwise well suited for the solution by the usual displacement method.

2. CLASSICAL PRIMAL FORMULATION

Let us consider field equations of linear elasticity, that is the constitutive equation:

$$\mathbf{T} - \mathbf{C}\mathbf{e}(\mathbf{u}) = \mathbf{0} \text{ in } \Omega, \quad (1)$$

strain–displacement relationship

$$2\mathbf{e}(\mathbf{u}) = \nabla\mathbf{u}^T + \nabla\mathbf{u}, \quad (2)$$

and the equilibrium equation

$$\text{div}\mathbf{T} + \mathbf{f} = \mathbf{0} \text{ in } \Omega. \quad (3)$$

In these expressions, \mathbf{T} is the symmetric stress tensor, \mathbf{u} the displacement vector, \mathbf{e} denotes the infinitesimal strain tensor, \mathbf{f} the vector of the body forces, \mathbf{C} the elasticity tensor and Ω is an open, bounded domain of the elastic body.

In order to find out unique solution of the above equations, a traction (Neumann) and geometric (kinematic, Dirichlet) boundary conditions should be defined:

$$\mathbf{T}\mathbf{n} - \mathbf{p} = \mathbf{0} \quad \text{on } \partial\Omega_t, \quad (4)$$

$$\mathbf{u} - \mathbf{w} = \mathbf{0} \quad \text{on } \partial\Omega_u, \quad (5)$$

where, \mathbf{n} is the unit normal vector to the boundary $\partial\Omega$, \mathbf{w} is the vector of the prescribed displacements and \mathbf{p} is the vector of the boundary tractions, while $\partial\Omega_u$ and $\partial\Omega_t$ are respectively the portions of the $\partial\Omega$ where displacements and stresses are prescribed.

Weak formulation of the *primal* problem, i.e. displacement method in the case of elasticity, is obtained by writing the equilibrium law in weak form and integrating by parts:

Find $\mathbf{u} \in H^1(\Omega)^n$ such that $\mathbf{u}|_{\partial\Omega_u} = \mathbf{w}$ and

$$\int_{\Omega} \mathbf{C} \mathbf{e}(\mathbf{u}) : \mathbf{e}(\mathbf{v}) d\Omega = \int_{\Omega} \mathbf{v} \cdot \mathbf{f} d\Omega + \int_{\partial\Omega_t} \mathbf{v} \cdot \mathbf{p} d\partial\Omega \quad (6)$$

for all $\mathbf{v} \in H^1(\Omega)^n$ such that $\mathbf{v}|_{\partial\Omega_u} = \mathbf{0}$.

Here, $H^1(\Omega)^n$ is the space of all vectorfields which are square integrable and have square integrable gradient and n is the number of spatial dimensions of the problem under consideration, while \mathbf{v} are the weight functions.

After the problem is defined in a weak form, some discretization technique should be introduced in order to find a solution over a finite dimensional space U_h of finite element solution \mathbf{u}_h .

From the above sketch of the classical finite element displacement method (CFE) it is obvious that stresses, see (1) and (2), although often most important quantities, have to be determined *a posteriori* by differentiation in post-processing part of finite element analysis which entails a loss of accuracy [1]. This is a serious drawback of the displacement finite element method and one of the main reasons for the introduction of the mixed finite element scheme as an alternative basis for studying the behaviour of continuous bodies.

3. PRESENT PRIMAL–MIXED FORMULATION

The weak form of a mixed problem, associated with Hellinger–Reissner variational principle [1,2] is used:

Find $\{\mathbf{u}, \mathbf{T}\} \in H^1(\Omega)^n \times L_2(\Omega)_{sym}^{n \times n}$ such that $\mathbf{u}|_{\partial\Omega_u} = \mathbf{w}$ and:

$$\int_{\Omega} (\mathbf{A} \mathbf{T} : \mathbf{S} - \mathbf{S} : \nabla \mathbf{u} - \nabla \mathbf{v} : \mathbf{T}) d\Omega = - \int_{\Omega} \mathbf{v} \cdot \mathbf{f} d\Omega - \int_{\partial\Omega_t} \mathbf{v} \cdot \mathbf{p} d\partial\Omega \quad (7)$$

for all $\{\mathbf{v}, \mathbf{S}\} \in H^1(\Omega)^n \times L_2(\Omega)_{sym}^{n \times n}$ such that $\mathbf{v}|_{\partial\Omega_t} = \mathbf{0}$.

In this expression $\mathbf{a} = \mathbf{c}^{-1}$ is the elastic compliance tensor, while \mathbf{S} are the weight functions. Space $L_2(\Omega)_{sym}^{n \times n}$ is the space of all symmetric tensorfields.

Because the displacement spaces are the same as in the classical displacement approach, and the stress space can be discontinuous at the element boundaries, it is a straightforward task to construct the elements of the above type. However, it is possible to consider also the continuous stress spaces, i.e. $\mathbf{T} \in (H^1)^{n \times n}$, the space of all symmetric tensorfields that have square integrable gradient. This approach has been successfully used by Mirza and Olson [3] for linear triangles and in [4] for bilinear isoparametric quadrilaterals, and the numerical results indicated high accuracy of a model. The problem of solvability of such configurations has been further elaborated in [2] and [5] by Zienkiewicz and Taylor *et al.* The next two steps in the development of a model were the introduction of stress constraints as essential boundary conditions [6], and stabilization of primal–mixed elements by full or partial hierarchic interpolation of stresses one order higher than displacements [7]. The main motivation for introduction of the boundary traction conditions as essential ones has been the further enhancement of the accuracy and appropriate modeling of the planes of symmetry. The accuracy of the formulation has been considered in [8], and the efficiency in [9]. The present paper is the first one considering the stability of the scheme more rigorously by the use of numerical inf–sup test [10,11,12].

3.1. Finite element subspaces

We let C_h be the partitioning of Ω into elements Ω_i and define the finite element subspaces for the displacement vector, the stress tensor and the appropriate weight functions respectively as:

$$\begin{aligned} U_h &= \{ \mathbf{u} \in (H^1)^n(\Omega) \mid \mathbf{u}|_{\partial\Omega_u} = \mathbf{w}, \mathbf{u}|_{\Omega_i} = U^K(\Omega_i)\mathbf{u}_K, \forall \Omega_i \in C_h \}, \\ V_h &= \{ \mathbf{v} \in (H^1)^n(\Omega) \mid \mathbf{v}|_{\partial\Omega_u} = \mathbf{0}, \mathbf{v}|_{\Omega_i} = V^K(\Omega_i)\mathbf{v}_K, \forall \Omega_i \in C_h \}, \\ T_h &= \{ \mathbf{T} \in (H^1)^{n \times n}(\Omega) \mid \mathbf{T} \cdot \mathbf{n}|_{\partial\Omega_t} = \mathbf{p}, \mathbf{T}|_{\Omega_i} = T_L(\Omega_i)\mathbf{T}^L, \forall \Omega_i \in C_h \}, \\ S_h &= \{ \mathbf{S} \in (H^1)^{n \times n}(\Omega) \mid \mathbf{S} \cdot \mathbf{n}|_{\partial\Omega_t} = \mathbf{0}, \mathbf{S}|_{\Omega_i} = S_L(\Omega_i)\mathbf{S}^L, \forall \Omega_i \in C_h \}. \end{aligned} \quad (8)$$

In these expressions \mathbf{u}_K and \mathbf{T}^L are the nodal values of the displacement vector \mathbf{u} and stress tensor \mathbf{T} respectively. Accordingly, U^K and T_L are the corresponding values of the interpolation functions, connecting the displacements and stresses at an arbitrary point in Ω_i (the body of an element), and the nodal values of these quantities. The complete analogy holds for the displacement and stress variations (weight functions) \mathbf{v} and \mathbf{S} respectively.

3.2. Compact matrix form of the FE equations

As it has been shown in [6], problem under consideration based on Equation (7) can be formulated in a symbolic matrix form as:

$$\begin{bmatrix} \mathbf{A} & -\mathbf{D} \\ -\mathbf{D}^T & \mathbf{0} \end{bmatrix} \begin{bmatrix} \mathbf{t} \\ \mathbf{u} \end{bmatrix} = - \begin{bmatrix} \mathbf{0} \\ \mathbf{f} + \mathbf{p} \end{bmatrix}. \quad (9)$$

In this expression \mathbf{t} and \mathbf{u} are the column matrices of the stress and displacement components nodal values. The members of the matrices \mathbf{A} and \mathbf{D} and of the vectors (column matrices) \mathbf{f} and \mathbf{p} (discretized body and surface forces) are respectively:

$$A_{\Lambda uv \Gamma st} = \sum_e \int_{\Omega_i} \Omega_\Lambda^N S_N g_{(\Lambda)u}^a g_{(\Lambda)v}^b A_{abcd} g_{(\Gamma)s}^c g_{(\Gamma)t}^d T_L \Omega_\Gamma^L d\Omega \quad (10)$$

$$D_{\Lambda uv}^{\Gamma q} = \sum_e \int_{\Omega_i} \Omega_\Lambda^N S_N U_a^K \Omega_K^\Gamma g_{(\Lambda)u}^a g_{(\Lambda)v}^{(\Gamma)q} d\Omega \quad (11)$$

$$f^{\Lambda q} = \sum_e \int_{\Omega_i} g_a^{(\Lambda)q} \Omega_\Lambda^M V^M f^a d\Omega \quad (12)$$

$$p^{\Lambda q} = \sum_e \int_{\partial\Omega_u} g_a^{(\Lambda)q} \Omega_\Lambda^M V^M p^a d\partial\Omega \quad (13)$$

where

$$g_{(L)s}^{(K)m} = \delta_{kl} g^{(K)mn} \frac{\partial z^k}{\partial x^{(K)m}} \frac{\partial z^l}{\partial y^{(L)s}}, \quad (14)$$

$$g_{(L)s}^a = \delta_{kl} g^{ab} \frac{\partial z^k}{\partial \xi^b} \frac{\partial z^l}{\partial y^{(L)s}}, \quad (15)$$

$$g_b^{(K)q} = \delta_{kl} g^{(K)qp} \frac{\partial z^k}{\partial \xi^b} \frac{\partial z^l}{\partial x^{(K)p}}. \quad (16)$$

are the Euclidean shifters. In this paper we will consider isotropic elastic examples where the compliance tensor components are of the form:

$$A_{abcd} = \frac{1}{2E} \left[(1+\nu)(g_{ca}g_{db} + g_{cb}g_{da}) - 2\nu g_{ab}g_{cd} \right] \quad (17)$$

In the above expressions z^i ($i, j, k, l = 1, 2, 3$) are the global Cartesian coordinates, while $x^{(K)n}$ ($m, n, p, q = 1, 2, 3$) and $y^{(L)s}$ ($r, s, t, u, v = 1, 2, 3$) are local (nodal) coordinates, used for determination of the nodal displacements and stresses respectively. Commonly used notions, ξ^a ($a, b, c, d = 1, 2, 3$) are taken for the

local (element) coordinates, usually convected (parametric, isoparametric). Further, $g^{(K)mn}$ and g^{ab} are the components of the contravariant fundamental metric tensors, the first one with respect to $x^{(K)n}$ and the second to ξ^b . Computation of these quantities is described in detail per instance in [7]. Furthermore, $U_a^K = \partial U^K / \partial \xi^a$. Also, A_{abcd} are the components of the elastic compliance tensor \mathbf{A} , while f^a and p^a are the body forces and boundary tractions, respectively. Integration is performed over the domain Ω_i of each element, or over the part of the boundary surface $\partial\Omega_{it}$ where the tractions are given, while summation is over all the elements of a system. Finally, Ω_M^Λ is a connectivity operator between global nodes Λ, Γ and element nodes K, M .

Because the tensorial character [13] of Equation (7) is fully respected, one can easily choose at each global node different coordinate systems for the stresses and/or displacements, for the most convenient application of boundary conditions and interpretation of output results.

It has been shown in [6] that Equation (9) can be decomposed for unknown (variable) and known (prescribed) values of the stresses and displacements denoted by the indices v and p respectively:

$$\begin{bmatrix} \mathbf{A}_{vv} & -\mathbf{D}_{vv} \\ -\mathbf{D}_{vv}^T & \mathbf{0} \end{bmatrix} \begin{bmatrix} \mathbf{t}_v \\ \mathbf{u}_v \end{bmatrix} = \begin{bmatrix} -\mathbf{A}_{vp} & \mathbf{D}_{vp} \\ \mathbf{D}_{pv}^T & \mathbf{0} \end{bmatrix} \begin{bmatrix} \mathbf{t}_p \\ \mathbf{u}_p \end{bmatrix} - \begin{bmatrix} \mathbf{0} \\ \mathbf{f}_p + \mathbf{p}_p \end{bmatrix} \quad (18)$$

In these expressions the nodal stresses t^{Lst} and displacements u_{Kq} components are consecutively ordered in the column matrices \mathbf{t} and \mathbf{u} respectively.

3.3. Solvability of a system

The Equation (18) can be rewritten in the simplified form:

$$\begin{bmatrix} \hat{\mathbf{A}} & -\hat{\mathbf{D}} \\ -\hat{\mathbf{D}}^T & \mathbf{0} \end{bmatrix} \begin{bmatrix} \hat{\mathbf{t}} \\ \hat{\mathbf{u}} \end{bmatrix} = \begin{bmatrix} \mathbf{q} \\ \mathbf{r} \end{bmatrix}. \quad (19)$$

Necessary conditions for the solvability of the above equation can be checked by the patch test of Zienkiewicz *et al.* [5], while the sufficient ones can be confirmed by the use of the eigenvalue analysis of Olson [14]. The results of these tests are given in the Tables 1–5. In these tables, all displacement degrees of freedom at node, i.e., $\{u_1, u_2\}$ are considered to be active and the *displacement node* is denoted by circle. The *stress nodes* with all three stress components $\{t^{11}, t^{12}, t^{22}\}$ active are denoted by the rectangular triangle. If only one stress component is active, the stress node is denoted by the appropriate dash, i.e., $\text{—} \{t^{11}, 0, 0\}$, $\text{\textbackslash} \{0, t^{12}, 0\}$, $| \{0, 0, t^{22}\}$.

3.3.1. Patch test

This simple test is useful in our case, because it helps to eliminate some of many combinations of stress interpolations and boundary conditions (Table 1–5). For the better readability, the element acronyms are taken from [5]. In these tables the degrees of freedom are counted in such a manner that, at common nodes, are divided by the number of adjacent elements (2 or 4). It is considered that the element (configuration) passes patch test if the number of the stress degrees of freedom n_t is greater than the number of displacements degrees of freedom n_u . From the Table 1 it is evident that although QC4/4 without essential stress boundary conditions satisfies necessary solvability conditions (configuration 4.5), introduction of any such condition makes configuration unsolvable (configurations 4.2–4.4). This has been the first [7] and perhaps the most *naïve* motivation for the introduction of higher order interpolation for stresses than for displacements in the present formulation.

3.3.2. Eigenvalue analysis

The next test, sufficient for the solvability, is eigenvalue analysis of the system matrix in Equation (19). Note that number of positive eigenvalues correspond to the number of stress degrees of freedom n_t . Total number of zero and negative eigenvalues is equal to the number of displacement degrees of freedom n_u (in our case $4 \times 2 = 8$). The results are shown also in Tables 1–5. Because free two-dimensional configurations are considered, the test is passed if the number of zero eigenvalues is 3 i.e., equal to the member of the rigid body degrees of freedom. If greater than 3, some mechanisms are present, and the problem can't be solved.

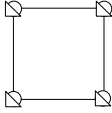
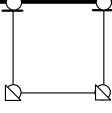
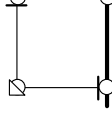
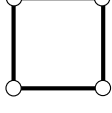
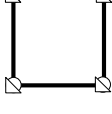
Element QC4/4		Primal–mixed finite element model stress and displacement bilinear approximation							
Configur- a-tion	Figure	Patch test[5]		status	Eigenvalues test [14]			Comment s	
		degrees of freedom			displacement	stress	status		
		n_t	n_u		modes	modes			
				$\lambda < 0$	$\lambda = 0$	$\lambda > 0$			
4.1		$\frac{12}{4}$	$\frac{8}{4}$	pass	–	–	–	–	Core building block
4.2		$\frac{10}{4}$	$\frac{12}{4}$	fail	–	–	–	–	Boundary building block
4.3		$\frac{7}{4}$	$\frac{18}{4}$	fail	–	–	–	–	Corner building block
4.4		0	$\frac{4 \times 2 - 3 = 5}{4}$	fail	–	–	–	–	Free element with stress boundary conditions
4.5		12	$\frac{4 \times 2 - 3 = 5}{4}$	pass	5	3	12	pass	Free element without stress boundary conditions

Table 1. Necessary and sufficient solvability tests. One–element configurations QC4/4

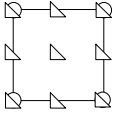
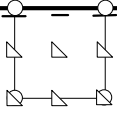
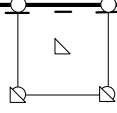
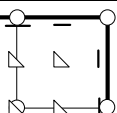
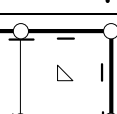
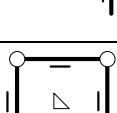
Element QC4/9	Primal–mixed finite element model								Comments
	displacement bilinear approximation				stress biquadratic approximation				
Configur- a- tion	Figure	Patch test[5]			Eigenvalues test [14]			status	
		Degrees of freedom		status	displacement modes		stress modes		
		n_t	n_u		$\lambda < 0$	$\lambda = 0$			$\lambda > 0$
9.1		$\frac{48}{4}$	$\frac{8}{4}$	pass	–	–	–	–	Core building block
9.2		$\frac{44}{4}$	$\frac{12}{4}$	pass	–	–	–	–	Boundary building block
9.3		$\frac{26}{4}$	$\frac{12}{4}$	pass	–	–	–	–	Boundary building block (restricted)
9.4		$\frac{39}{4}$	$\frac{18}{4}$	pass	–	–	–	–	Corner building block
9.5		$\frac{27}{4}$	$\frac{18}{4}$	pass	–	–	–	–	Corner building block (restricted)
9.6		7	$\frac{4 \times 2 - 3 = 5}{4}$	pass	5	3	7	pass	Free element with stress boundary conditions

Table 2. Necessary and sufficient solvability tests. One–element configurations QC4/9

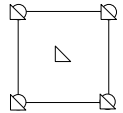
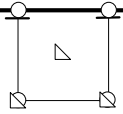
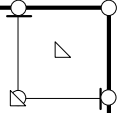
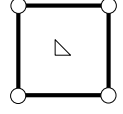
Element QC4/5		Primal–mixed finite element model displacement bilinear approximation, stress biquadratic approximation (<i>bubble</i> only)							
Configu- ration	Figure	Patch test [5]			Eigenvalues test [14]			Comments	
		Degrees of freedom		status	displacement modes		stress modes		status
		n_t	n_u		$\lambda < 0$	$\lambda = 0$			
5.1		$\frac{24}{4}$	$\frac{8}{4}$	pass	–	–	–	–	Core building block
5.2		$\frac{22}{4}$	$\frac{12}{4}$	pass	–	–	–	–	Boundary building block
5.3		$\frac{19}{4}$	$\frac{18}{4}$	pass	–	–	–	–	Corner building block
5.4		3	$\frac{4 \times 2 - 3 = 5}{3 = 5}$	fail	3	5	3	fail	Free element with stress boundary conditions

Table 3. Necessary and sufficient solvability tests. One–element configurations QC4/5

Primal–mixed finite element model													
configu- ration	Figure	Patch test [5]			Eigenvalues test [14]			status	Comments				
		Degrees of freedom		status	displaceme nt modes		stress modes						
		n_t	n_u		$\lambda < 0$	$\lambda = 0$				$\lambda > 0$			
1	<table border="1"><tr><td>4.1</td><td>4.1</td></tr><tr><td>4.1</td><td>4.1</td></tr></table>	4.1	4.1	4.1	4.1	27	18–3 =15	pass	15	3	27	pass	QC4/4 without stress boundary conditions
4.1	4.1												
4.1	4.1												
2	<table border="1"><tr><td>9.4</td><td>9.4</td></tr><tr><td>9.4</td><td>9.4</td></tr></table>	9.4	9.4	9.4	9.4	39	18–3 =15	pass	15	3	27	pass	QC4/9 Taylor– Hood type element with stress boundary conditions
9.4	9.4												
9.4	9.4												
3	<table border="1"><tr><td>9.5</td><td>9.5</td></tr><tr><td>9.5</td><td>9.5</td></tr></table>	9.5	9.5	9.5	9.5	27	18–3 =15	pass	15	3	27	pass	QC4/9
9.5	9.5												
9.5	9.5												
4	<table border="1"><tr><td>5.3</td><td>5.3</td></tr><tr><td>5.3</td><td>5.3</td></tr></table>	5.3	5.3	5.3	5.3	19	18–3 =15	Pass	13	5	19	fail	QC4/5 Two mechanism s
5.3	5.3												
5.3	5.3												

Table 4. Necessary and sufficient solvability tests. 2×2 element configurations

Primal–mixed finite element model																		
configu- ration	Figure	Patch test [5]			Eigenvalues test [14]			status	Comments									
		Degrees of freedom		status	displaceme nt modes	stress modes												
		n_t	n_u			$\lambda < 0$	$\lambda = 0$			$\lambda > 0$								
1	<table border="1"><tr><td>4.1</td><td>4.1</td><td>4.1</td></tr><tr><td>4.1</td><td>4.1</td><td>4.1</td></tr><tr><td>4.1</td><td>4.1</td><td>4.1</td></tr></table>	4.1	4.1	4.1	4.1	4.1	4.1	4.1	4.1	4.1	48	32–3 =29	pass	29	3	48	pass	QC4/4 without stress boundary conditions
4.1	4.1	4.1																
4.1	4.1	4.1																
4.1	4.1	4.1																
2	<table border="1"><tr><td>9.4</td><td>9.2</td><td>9.4</td></tr><tr><td>9.2</td><td>9.1</td><td>9.2</td></tr><tr><td>9.4</td><td>9.2</td><td>9.4</td></tr></table>	9.4	9.2	9.4	9.2	9.1	9.2	9.4	9.2	9.4	95	32–3 =29	pass	29	3	95	pass	QC4/9 Taylor– Hood type element with stress boundary conditions
9.4	9.2	9.4																
9.2	9.1	9.2																
9.4	9.2	9.4																
3	<table border="1"><tr><td>9.5</td><td>9.3</td><td>9.5</td></tr><tr><td>9.3</td><td>5.1</td><td>9.3</td></tr><tr><td>9.5</td><td>9.3</td><td>9.5</td></tr></table>	9.5	9.3	9.5	9.3	5.1	9.3	9.5	9.3	9.5	59	32–3 =29	pass	29	3	59	pass	QC4/5 QC4/9
9.5	9.3	9.5																
9.3	5.1	9.3																
9.5	9.3	9.5																
4	<table border="1"><tr><td>9.5</td><td>5.2</td><td>9.5</td></tr><tr><td>5.2</td><td>5.1</td><td>5.2</td></tr><tr><td>9.5</td><td>5.2</td><td>9.5</td></tr></table>	9.5	5.2	9.5	5.2	5.1	5.2	9.5	5.2	9.5	55	32–3 =29	pass	29	3	55	pass	QC4/5 QC4/9
9.5	5.2	9.5																
5.2	5.1	5.2																
9.5	5.2	9.5																
5	<table border="1"><tr><td>9.5</td><td>5.2</td><td>9.5</td></tr><tr><td>5.2</td><td>4.1</td><td>5.2</td></tr><tr><td>9.5</td><td>5.2</td><td>9.5</td></tr></table>	9.5	5.2	9.5	5.2	4.1	5.2	9.5	5.2	9.5	52	32–3 =29	pass	29	3	52	pass	QC4/4 QC4/5 QC4/9
9.5	5.2	9.5																
5.2	4.1	5.2																
9.5	5.2	9.5																

Table 5. Necessary and sufficient solvability tests. 3×3 element configurations

3.4. Stability. Inf–sup test.

The finite element is stable if it satisfy two necessary conditions for stability in Brezzi’s theory [11]. The first Brezzi’s condition is ellipticity requirement and the second one is the inf–sup test. In the present case the first Brezzi’s condition is automatically satisfied, since according to [1] primal–mixed formulation automatically satisfies the ellipticity on the kernel.

The element considered here can be in fact identified as an application of the quadrilateral Taylor–Hood type element in elasticity (Brezzi and Fortin [15], p.284, example 3.3), where it has been said: “*It is not known if this element is stable*”. Hence it has been decided to use inf–sup test of Chapelle and Bathe [10] to check the stability of some configurations considered. The numerical inf–sup test will be satisfied if for the meshes of increasing density, value μ_{\min} :

$$\mu_{\min} = \inf_{\mathbf{u} \in H^1} \sup_{\mathbf{T} \in L^2} \frac{b(\mathbf{T}_h, \mathbf{u}_h)}{\|\mathbf{T}_h\| \|\mathbf{u}_h\|} \quad (20)$$

remains bounded above zero. The entries in Equation (20) can be defined as:

$$b(\mathbf{T}_h, \mathbf{u}_h) = \sum_e \int_{\Omega_e} \mathbf{T}_h : \nabla \mathbf{u}_h \, d\Omega_e, \quad (21)$$

$$\|\mathbf{T}_h\|^2 = \sum_e \int_{\Omega_i} \mathbf{T}_h : \mathbf{T}_h d\Omega, \quad (22)$$

$$\|\mathbf{u}_h\|^2 = \sum_e \int_{\Omega_i} \nabla \mathbf{u}_h^T : \nabla \mathbf{u}_h d\Omega. \quad (23)$$

In the present context the energy norms were used rather than L_2 ones, Equations (22) and (23):

$$\|\mathbf{T}_h\|_U^2 = \sum_e \int_{\Omega_i} \mathbf{A} \mathbf{T}_h : \mathbf{T}_h d\Omega, \quad (24)$$

$$\|\mathbf{u}_h\|_U^2 = \sum_e \int_{\Omega_i} \nabla \mathbf{u}_h^T : \mathbf{C} \nabla \mathbf{u}_h d\Omega. \quad (25)$$

For the practical reasons one can rewrite these expressions in a matrix form:

$$b(\mathbf{T}_h, \mathbf{u}_h) = \mathbf{t}^T \mathbf{D} \mathbf{u}, \quad (26)$$

$$\|\mathbf{T}_h\|^2 = \mathbf{t}^T \mathbf{A}_0 \mathbf{t}, \quad (27)$$

$$\|\mathbf{u}_h\|^2 = \mathbf{u}^T \mathbf{K}_0 \mathbf{u}, \quad (28)$$

$$\|\mathbf{T}_h\|_U^2 = \mathbf{t}^T \mathbf{A} \mathbf{t}, \quad (29)$$

$$\|\mathbf{u}_h\|_U^2 = \mathbf{u}^T \mathbf{K} \mathbf{u}. \quad (30)$$

In the last expression, the elements of the *stiffness matrix* \mathbf{K} of the classical primal formulation (6) are given by:

$$K^{\Lambda m \Gamma n} = \sum_e \Omega_L^\Lambda \int_{\Omega_i} g_a^{(\Lambda)m} U_b^L C^{abcd} U_d^K g_c^{(\Gamma)n} d\Omega \Omega_K^\Gamma \quad (31)$$

where for the isotropic elastic material in plane stress problems:

$$C^{abcd} = \frac{E}{2(1-\nu^2)} \left[2\nu g^{ab} g^{cd} + (1-\nu)(g^{ac} g^{bd} + g^{ad} g^{bc}) \right] \quad (32)$$

Note that for the calculation of \mathbf{A}_0 and \mathbf{K}_0 one can use the same routines as for \mathbf{A} and \mathbf{K} respectively, choosing $E=1$ and $\nu=0$ in the expressions (17) and (32). However, at least for this particular problem, there is a negligible change of the numerical value of μ_{\min} , when \mathbf{A} and \mathbf{K} are replaced by \mathbf{A}_0 and \mathbf{K}_0 respectively.

We determine μ_{\min} , the smallest eigenvalue of the generalized eigenvalue problem as it is defined by Brezzi [11], p.76, Equation (3.22), or Babuska [12], p.14. In matrix notations:

$$\mathbf{D}^T \mathbf{A}^{-1} \mathbf{D} \mathbf{u}_i = \mu_i^2 \mathbf{K} \mathbf{u}_i. \quad (33)$$

The geometry of the test problem considered (Fig. 1) is the same as in Chapelle and Bathe [10]. The results from [24] are given in the Figure 2. The points at this figure correspond to configurations defined in Tables 1–5. To be more specific, one–element point on the line QC4/4 corresponds to Configuration 4.5 (Table 1), while 2×2 and 3×3 cases are given as configuration 1, Tables 4 and 5 respectively. Additional configurations (4×4 and 5×5) are constructed by the expansion of 3×3 configurations, retaining the same type of core, side and corner blocks. Similarly, one–element configuration corresponding to lines QC4/9 and QC4/9+ QC4/5 can be found in Table 2, as 9.6, while multi–element configurations are defined as cases 2 and 3 respectively, Tables 4 and 5.

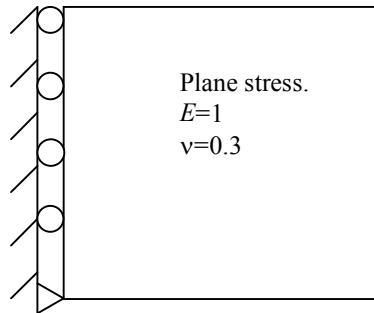


Fig.1. Inf–sup test model considered.

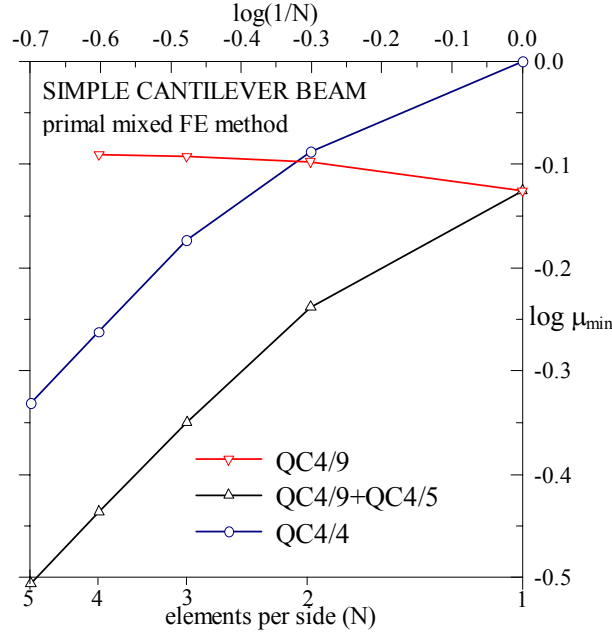


Fig. 2. Inf–sup results, primal–mixed elements.

From the above analysis it follows that the primal–mixed Taylor–Hood type quadrilateral element in elasticity QC4/9, at least for the configuration considered, is stable even in the presence of essential stress boundary conditions. This is an important result, because theoretical bounds for inf–sup value in this case are lacking [15].

Unfortunately, various more economical restrictions of the above formulation, albeit solvable, are not proven to be stable. Nevertheless, these formulations, at least in the case of smooth enough boundary conditions, are highly accurate and converge with the optimal convergence rate.

4. NUMERICAL EXAMPLES

In order to illustrate the main properties of the present primal–mixed finite element method two–dimensional plane stress linear isotropic elastic model problem were examined.

The present procedure has been compared with the classical displacement type procedure (element Q4) based on a primal scheme. In the case of the displacement procedure calculations of stresses were done *a posteriori* (in post–processing part of finite element analysis) either with local stress smoothing by averaging the stresses at global nodes (QC4avg) or by the global L_2 projection procedure [17].

Due to (9) twice the strain energy U_h of finite element solution can be calculated in matrix form by:

$$2U_h = \mathbf{t}^T \mathbf{A} \mathbf{t}. \quad (34)$$

The popularity of this measure is partially due to a fact that it is, at a system level, equal to the work of the external forces W :

$$2W_h = \mathbf{u}^T [\mathbf{f} + \mathbf{p}] \quad (35)$$

which is even easier to calculate.

For the energy error determination in this paper we will use the expressions of the type

$$\eta = \frac{|2U - 2U_h|}{|2U|} \cdot 100\% \quad (36)$$

representing *relative percentage error* [18] or *precision* [19], where U is the exact or estimated strain energy.

4.1. Cook's membrane problem

The well known Cook's membrane problem [20] is shown in the Fig. 3. This problem is useful for the comparative study of accuracy because there are available numerical results from other sources.

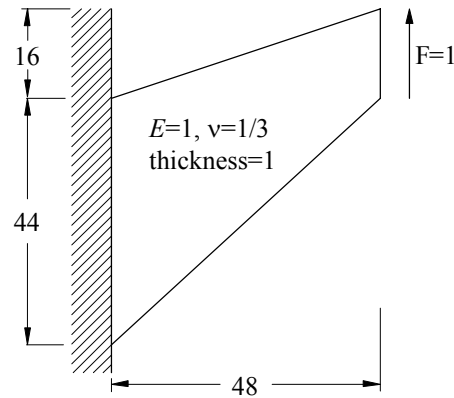


Fig. 3. Cook's membrane problem.

In the Table 6 numerical results for the vertical displacements $u_y(P)$ at node P(48,52), calculated by the displacement method (element Q4) and present method (QC4/5), are compared with Q6 (Taylor–Wilson) [21] and Q4I (Kojic *et.al.*) [22]:

Normalized displacements at the centre of the tip section			
estimated converged value 23.96 [23]			
Element model	Number of elements per side		
	4	8	16
Q4	0.766	0.923	0.979
Q6	0.980	0.993	0.998
Q4I	0.973	0.988	0.997
QC4/5	0.982	0.998	1.001

Table 6. Necessary and sufficient solvability tests. 3×3 element configurations

Present model problem is also interesting because there is a stress singularity at the point D. The behaviour of the normal stress component, parallel to the edge CD, for the mesh 32×32 is shown in Figures 4 and 5. Note that the stress behaviour near singularity, which is somewhat oscillatory for QC4/4 scheme, is smoothed by the use of QC4/5 scheme. The stress boundary conditions for the model QC4/5 are enforced at each node except at the singularity D. Note that the oscillatory behaviour is one of main complaints about the continuous stress formulation [5]. However, the present results indicate that this behaviour is not a necessary consequence of the continuous stress formulation, but rather an indication of the unstable behaviour of the configuration considered. In fact, the enrichment of a stress space towards the stable one (QC4/9) eliminates stress oscillations. It also should be noted that stress oscillations tend to be more pronounced for the denser meshes, which is in the direct correlation with the decrease of inf–sup value. Hence, the *stability* is an ultimate reason requiring the proper enrichment of the stress space.

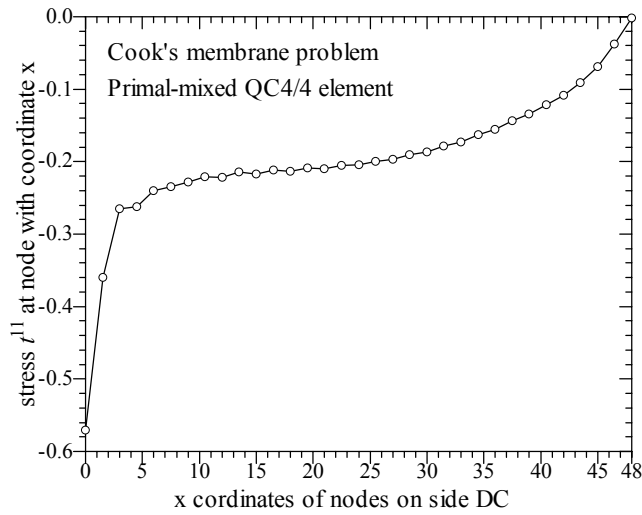


Fig. 4. Element QC4/4 – behaviour in the presence of singularity.

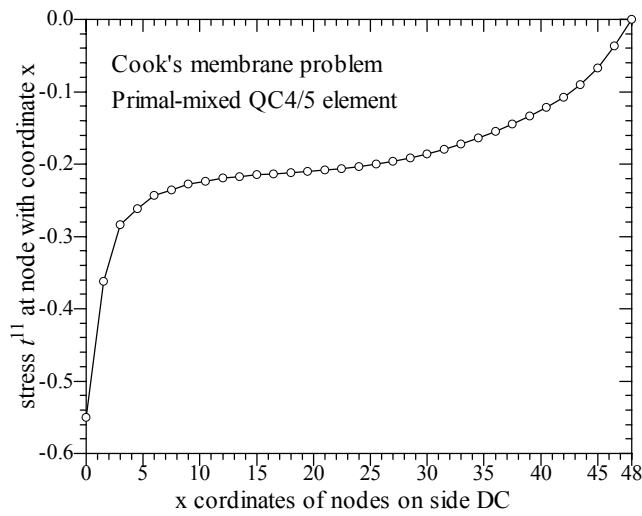


Fig. 5. Element QC4/5 – behaviour in the presence of singularity.

4.2. Uniformly loaded ring

For the purpose of the comparison of present results with some analytical solutions, a problem of a thin uniformly loaded ring (Lamé, 1852) by the internal pressure of 10 units, shown in Fig. 6, is considered. The internal diameter of a ring has 5 and the external one 20 units. Material characteristics are given by the Young modulus $E=1$ and Poisson's ratio $\nu=0.3$. The thickness of the ring is 1. Exact value of strain energy is $U = 1.791666 \int_0^{\theta} d\theta$, and for $\theta=\pi/2$ strain energy has the value

$U=2.814343$, where angle θ is angle between the sides AB and CD. Circular stress is positive and its maximum value is on the internal contour, $t_{\theta\theta} = 11.3333333$.

By taking advantage of symmetry of the model and in the case of the present primal–mixed scheme possibility of defining homogeneous and non–homogeneous boundary conditions in arbitrary coordinate systems, only one slice of elements is considered. For model with n elements, inner angle has value $\theta = \pi / 2n$.

For the proper simulation of the symmetry in such problems, it is necessary not only to adjust the displacement boundary conditions, but also the boundary tractions. This is also an important motivation for the introduction of the essential stress boundary conditions into the computational scheme.

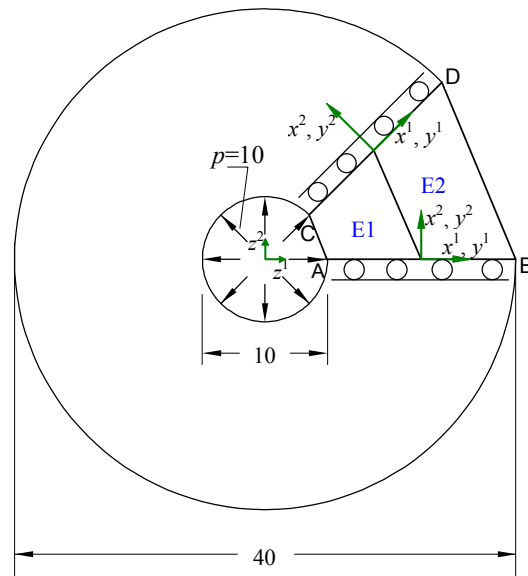


Fig. 6. Uniformly loaded ring – model problem.

Finite element models with 2^n elements are examined, where $n=1,2,3,4,5,6,7,8,9,10$. Because only one row of elements is considered the mesh with $2^{10}=1024$ elements is equivalent to the complete (circular) model with $4 \times 1024 \times 1024 = 4,194,304$ elements, or more than 20 million DOF (degrees of freedom). Hence, this model is a convenient example to give an impression about the number of significant digits obtainable by the use of very fine meshes, see Table 7.

Uniformly loaded ring – primal mixed method number of elements QC4/5 in slice is 2^n			
n	$t^{22}(A)$	strain energy U	ndof
1	.97551695546E+01	.25721519285E+01	20
2	.10351126161E+02	.26934190217E+01	38
3	.10946698017E+02	.27729614576E+01	74
4	.11210658629E+02	.28023889704E+01	146
5	.11298567195E+02	.28111419026E+01	290
6	.11324057751E+02	.28135156219E+01	578
7	.11330936082E+02	.28141329872E+01	1154
8	.11332723859E+02	.28142903721E+01	2306
9	.11333179671E+02	.28143301021E+01	4610
10	.11333294754E+02	.28143400827E+01	9218
<i>exact</i>	.11333333333E+02	.28143434188E+01	∞

Table 7: Uniformly loaded ring – numerical results QC4/5

The stress convergence at the inner boundary (node A) versus number of elements is shown in the Fig. 7. This figure illustrates a fact that the results with the complete quadratic stress distribution (QC4/9) are less accurate than with only central *bubble* retained (QC4/5). However, from the Fig. 8 it is evident that the configuration QC4/5 is unstable while QC4/9 is stable. Fortunately, at least in this particular problem instability does not influence convergence (Fig. 8). This behaviour should probably be attributed to the very regular boundary conditions, see [12], p.12 and [25] p.135.

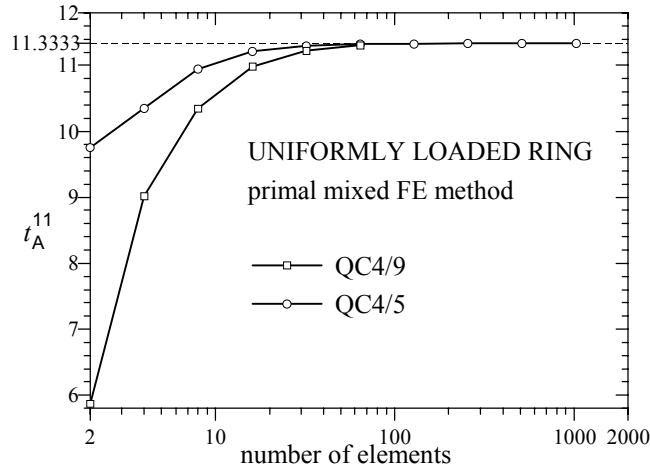


Fig. 7. Uniformly loaded ring stress convergence at A.

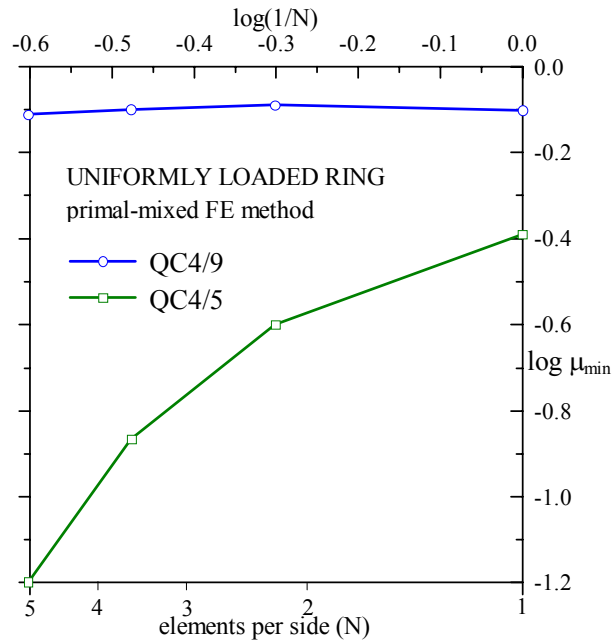


Fig. 8. Inf-sup results, elements QC4/5 and QC4/9.

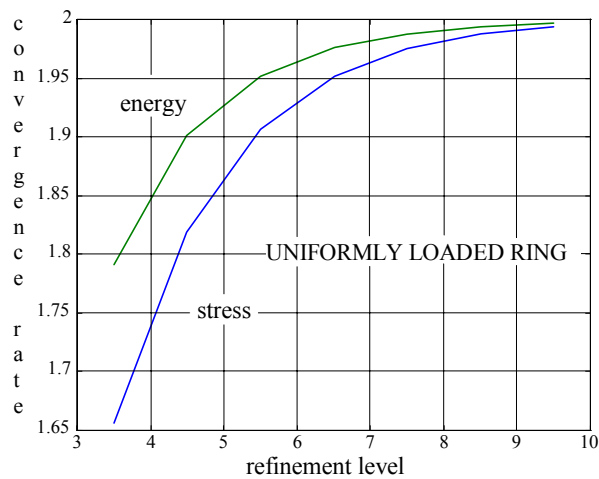


Fig. 9. Uniformly loaded ring (QC4/5). Asymptotic behaviour of the stress and energy convergence rates.

4.3. The square plate with a circular hole

The efficiency of the procedure is studied by the use of a typical regular two-dimensional example. This problem of the square plate with a circular hole [26] is depicted in Fig. 10. Only a quarter of it is analyzed due to the symmetry of that system. Isotropic, homogeneous material properties and the plane stress behavior are assumed. Modulus of elasticity and Poisson's coefficient have been taken to be $E=1$ and $\nu=0.3$. The numerical studies were made for the sequence of meshes with regularly increasing number of elements along the sides (Fig. 10).

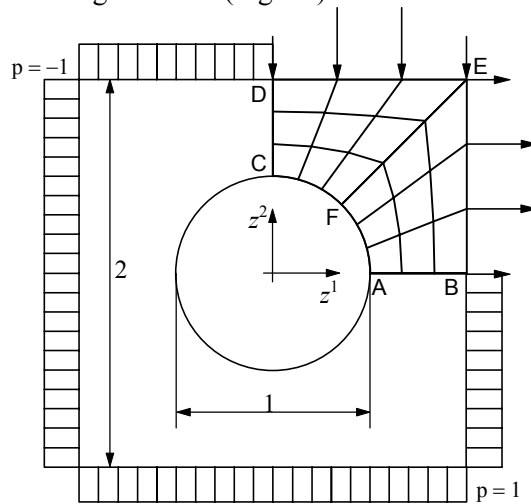


Fig. 10. Plate with a circular hole.

In this example configuration QC4/5.2+QC4/4.1 means that boundary building blocks 5.2 (Table 3) are used at the free boundaries (A–C and B–E–D), while 4.1 (Table 1) are used as core blocks. Note that at the planes of symmetry (D–C and A–B) both stress and displacement symmetry conditions are exactly satisfied. The description of the case QC4/5.2+QC4/5.1 is analogous. For the configuration QC4/4 the stress boundary conditions at the free boundaries are not satisfied. However, the symmetry conditions are exactly satisfied again.

In Fig. 11 relative strain energy error norms (36) related to the time of execution are compared.

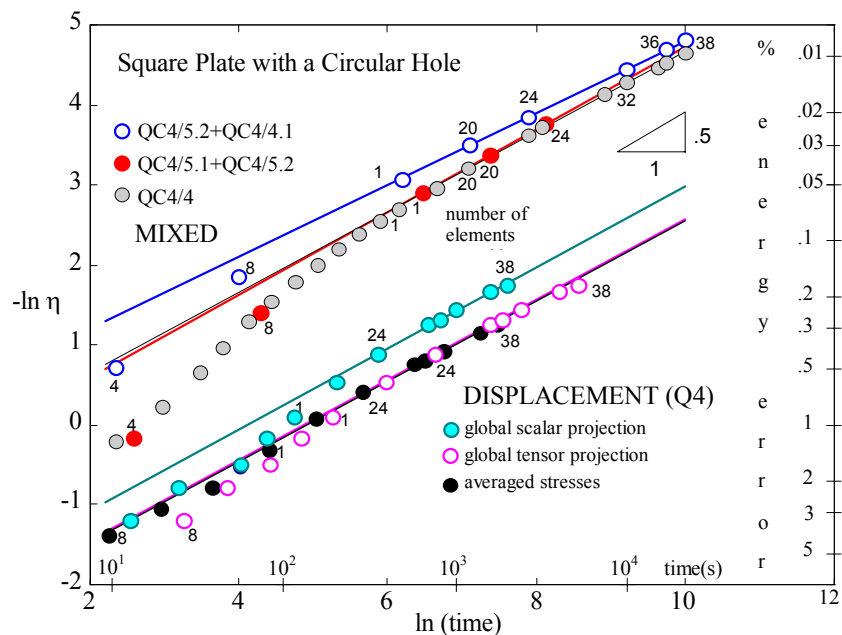


Fig. 11. Percentage error versus execution time.

From the Fig. 11 it can be concluded that the case with the stress *bubble* nodes located only in elements along a physical boundary (QC4/5+QC4/4) is more efficient than the case when we have bubble nodes in all elements (QC4/5), and also than the simple bilinear approach (QC4/4) without boundary traction conditions applied. Anyhow, all these approaches are clearly superior compared with the classical analysis (Q4), irrespectively on the method of postprocessing used in that procedure. The configurations in this example are not proven to be stable in the sense of the second Brezzi's condition. However, these are extremely efficient. Few preliminary results with stable QC4/9 (Taylor–Hood) configuration, and the corresponding operational counts, indicate that the efficiency of this formulation should lie close to the mean value of the graphs shown at the Fig. 11.

5. CONCLUSIONS

In the present paper a solution procedure of the primal–mixed finite element equations based on the Reissner's principle has been presented. On the basis of the above analysis and the numerical results one can conclude, first, that the mixed elements with complete continuity can be practically realized, second, that simple and clear measures for the enhancement of the stability of a solution of the resulting equations are available. One of the most important results of the present paper is the numerical proof of stability of the primal–mixed Taylor–Hood type interpolation. It has also been shown that some configurations, not stable in the LBB sense, can be extremely efficient, at least in the case of smooth boundary conditions. It remains for the further work to search for the best possible primal–mixed schemes, satisfactory from both the stability and efficiency points of view.

REFERENCES

1. Arnold D.N., (1990) *Mixed finite element methods for elliptic problems*, Computer Methods in Applied Mechanics and Engineering, N^o 82, pp. 281–300.
2. Zienkiewicz O.C. and Taylor R.L., (1989) *The Finite Element Method, VOL I*, McGraw-Hill, London.
3. Mirza F.A. and Olson M.D., (1980) *The mixed finite element in plane elasticity*, International Journal of Numerical Methods in Engineering, N^o 15, pp. 273–289.
4. Berkoviæ M. and Draškoviæ Z., (1984) *Stress continuity in the finite element analysis*, in *Accuracy, Reliability and Training in FEM Technology*, ed. J. Robinson, Robinson and Associates, , pp. 110–118.
5. Zienkiewicz O.C., Zhu J.Z., Taylor R.L. and Nakazawa S., (1986) *The patch test for mixed formulations*. International Journal of Numerical Methods in Engineering, N^o 23, pp. 1873–1883.
6. Berkoviæ M. and Draškoviæ Z., (1991) *On the essential mechanical boundary conditions in two-field finite element approximations*, Computer Methods in Applied Mechanics and Engineering, N^o 91, pp. 1339–1355.
7. Berkoviæ M. and Draškoviæ Z.V., (1994) *A two-field finite element model related to the Reissner's principle*, Theoretical and Applied Mechanics, N^o 20, pp. 17–36.
8. Berkoviæ M., Draškoviæ Z. and Mijuca D., (1998) *A direct block sparse solution of the mixed finite element equations*, Computer Assisted Mechanics and Engineering Sciences, N^o 5, pp. 21–30.
9. Berkoviæ M. and Mijuca D., (1998) *An efficient continuous stress mixed model based on the Reissner's principle*, Fourth World Congress on Computational Mechanics, Buenos Aires.
10. Chapelle D. and Bathe K.J., (1993) *The inf-sup test*, Computers & Structures, N^o 47, vol. 4/5, pp. 537–545.
11. Brezzi F. and Fortin M., (1991) *Mixed and Hybrid Finite Element Methods*, Springer-Verlag, New York.
12. Babuska I., On the inf-sup (Babuska-Brezzi) condition, *TICAM Forum* #5, October 1996.
13. Draškoviæ Z., (1988) *On invariance of finite element approximations*, *Mechanika Teoretyczna i Stosowana*, N^o 26, pp. 597–601.
14. Olson M.D., (1983) *The mixed finite element method in elasticity and elastic contact problems*, in S.N. Atluri, R.H. Gallagher and O.C. Zienkiewicz, eds., *Hybrid and Mixed Finite Element Methods*, John Wiley & Sons, pp. 19–49.
15. Brezzi F. and Fortin M., (1993) *Mixed finite element methods with continuous stresses*, *Mathematical Models and Methods in Applied Sciences*, N^o 3, vol. 2, pp. 275–287.
16. Axelsson O. and Barker V.A., (1984) *Finite element solution of boundary value problem*, Accademic Press.
17. Mijuca D., Draškoviæ Z. and Berkoviæ M., (1996) *Displacement Based Stress Recovery Procedure*, *Advances in Finite Element Technology*, Civil-Comp Press, pp. 127–134.
18. Zienkiewicz O.C. and Zhu J.Z., (1987) *A simple error estimator and adaptive procedure for practical engineering analysis*, International Journal of Numerical Methods in Engineering, N^o 24, pp. 337–357.
19. Becker P. and Zhong H.G., (1994) *Mesh adaption for two dimensional stress analysis*, *Advances in Post and Preprocessing for Finite Element Technology*, Civil-Comp Press, pp. 47–59.

20. Cook R., (1974) *Improved two-dimensional finite element*, Journal of the Structural Division ASCE 100, pp. 1851–1861.
21. Stolarski H.K. and Chen Y.-I., (1995) *Assumed strain formulation for the four node quadrilateral with improved in-plane behaviour*, *International Journal of Numerical Methods in Engineering*, N^o38, pp. 1287–1305.
22. R. Slavkoviæ, M. Zivkoviæ and M. Kojiæ, (1994) *Enhanced 8-node three-dimensional solid and 4-node shell elements with incompatible generalized displacements*, *Communications in Numerical Methods in Engineering*, N^o10, pp. 699-709.
23. Canarozzi A.A., Canarozzi M., (1995) *A displacement scheme with drilling degrees of freedom for plane elements*, *International Journal of Numerical Methods in Engineering*, N^o38, pp. 3433–3452.
24. Mijuca D. (1999) *Primal-mixed finite element approach in solid mechanics*, Ph.D. Thesis, Faculty of Mathematics, University of Belgrade, (in Serbian).
25. Carey G. and Oden J.T., (1983) *Finite Elements: A Second Course*, Prentice-Hall, Englewood Cliffs.
26. Rao A.K, Raju I.S. and Krishna Murty A.V., (1971) *A powerful hybrid method in finite element analysis*, *IJNM in engineering*, N^o 3, pp. 389–403.